



Flight Test Results of the Microgravity Active Vibration Isolation System in China's Tianzhou-1 Mission

Wei Liu^{1,2} · Yang Gao¹ · Wenbo Dong¹ · Zongfeng Li¹

Received: 7 February 2018 / Accepted: 30 September 2018 / Published online: 26 October 2018
© The Author(s) 2018

Abstract

The Microgravity Active vibration Isolation System (MAIS) was operated on China's first cargo-spacecraft Tianzhou-1, which was launched on April 20, 2017 and re-entered atmosphere and burned on September 22, 2017. In this article, the flight test results of MAIS is presented. The results are evaluated in terms of the performances of microgravity acceleration and vibration attenuation under control. Firstly, the system configuration of MAIS on Tianzhou-1 is described, including operating modes, acceleration measurement, and control schemes. Then, two control performance indices, namely, microgravity acceleration and vibration attenuation, are introduced, followed by their definitions and methods of calculation. Subsequently, the flight test results of MAIS are described in detail. The microgravity acceleration under a PID (Proportional-Integral-Derivative) controller is at the order of $10^{-7} - 10^{-6} \text{ m/s}^2$ in the frequency band of 0.01–10 Hz, and the performance of vibration attenuation reaches -20 dB at frequencies higher than 0.2 Hz. The flight test results show that MAIS in the TZ-1 mission performed well and achieved the expected control performance of microgravity vibration isolation in orbit. Finally, some experiences and lessons learned are summarized, which can serve as a benchmark reference to develop MAIS-like devices on board China's Space Station in the near future.

Keywords Microgravity active vibration isolation system · Microgravity acceleration performance · Vibration attenuation performance · Tianzhou-1 cargo-spacecraft

Abbreviations

2D-PSD	Two-dimensional position sensitive detector
ARIS	Active rack isolation system
EXPRESS	Expedite the processing of experiments to the space station
FCE	Facility core element
g-LIMIT	Glovebox integrated microgravity isolation technology
ISPR	International standard payload rack

MAIS	Microgravity active vibration isolation system
MIM	Microgravity vibration isolation mount
MIMBU	Microgravity vibration isolation mount base unit
MSG	Microgravity science glovebox
MVIS	Microgravity vibration isolation subsystem
STABLE	Suppression of transient accelerations by levitation
STS	Space transportation system
TISS	Test of inverse-square-law in space (the payload for this test project)
TZ-1	TianZhou-1 cargo-spacecraft
TG-2	TianGong-2 manned space laboratory

This article belongs to the Topical Collection: Approaching the Chinese Space Station - Microgravity Research in China
Guest Editors: Jian-Fu Zhao, Shuang-Feng Wang

✉ Wei Liu
liuwei@csu.ac.cn

¹ Key Laboratory of Space Utilization, Technology and Engineering Center for Space Utilization, Chinese Academy of Sciences, Beijing 100094, China
² University of Chinese Academy of Sciences, Beijing 100049, China

Introduction

Spaceflight provides a long-term microgravity environment and eventually lays a solid foundation for the development of microgravity science and technology. Scientists have performed numerous scientific experiments in space by using



Fig. 1 Principle of microgravity active vibration isolation system

spacecraft, especially on the former Soviet Union's MIR space station and ISS (International Space Station). It is early to find that some scientific space experiments require a high-level microgravity environment. However, a space station often fails to provide satisfactory microgravity conditions owing to the presence of disturbing accelerations caused by several factors, such as crew activity, attitude maneuver, and motor vibration. Therefore, the amplitude of disturbing accelerations must be attenuated for the actualization of desired microgravity levels. The microgravity active vibration isolation system provides an effective approach for vibration attenuation in space, which can isolate from the vibration on spacecraft effectively and provide a high-level microgravity environment for scientific experiments. Microgravity acceleration performance index and vibration attenuation performance index are two design requirements for the microgravity active vibration isolation system. The former refers to the microgravity level requirement provided by the microgravity vibration isolation system, and the latter refers to the attenuation requirement of the acceleration of the vibration isolation platform relative to the acceleration of the spacecraft platform. The microgravity acceleration performance index is determined by microgravity science experiments, and the vibration attenuation performance index is determined by the microgravity acceleration performance index and the estimated disturbance level of the spacecraft platform. In order to achieve these two performance indexes, the design requirements of the sensor

measurement precision, the actuator output force precision and the control system bandwidth are proposed. Detailed description of the microgravity acceleration performance index and the vibration attenuation performance index, including their definition, can be seen in “[Microgravity performance indices in flight test](#)” section. The typical system is usually composed of a stator and a floater, and the principle of the system is depicted in Fig. 1. The stator is fixed on the spacecraft and the floater is levitated by electromagnetic force. The floater senses its microgravity acceleration and relative motion with respect to the stator, and these two errors are then treated as feedback information to a controller. The controller calculates the required forces and torques generated by electromagnetic actuators to attenuate the disturbing accelerations from the stator.

Several microgravity active vibration isolation systems have been developed, and most of them have been tested in space (Grodsinsky and Whorton 2000). ARIS, STABLE, and g-LIMIT were developed by NASA (National Aeronautics and Space Administration). The goal of ARIS (NASA 2005) was to isolate microgravity sensitive science experiments mounted in the ISPR by isolating the entire rack via an active control system. The active control system consists of inertial accelerometers mounted in the rack and voice-coil type actuators with integral position sensors placed between the rack and the space station. The ARIS was designed to isolate all frequencies greater than 0.01 Hz, and it was more effective in the 0.05 to 300 Hz range. In October 1995 STABLE (Edberg et al. 1996) was the first microgravity active vibration isolation device in space for microgravity science payloads on STS-73. STABLE provided component-level isolation as an alternative to the rack-level approach. The objective of STABLE was to demonstrate vibration isolation on-orbit with an operating scientific experiment, while passing power, data, and other services over some umbilical links. g-LIMIT (Whorton 2001) was a component-level isolation system for MSG on the ISS. It was designed around three

Fig. 2 Vibration attenuation performance of active vibration isolation systems (the data in this figure were estimated on the existing studies)

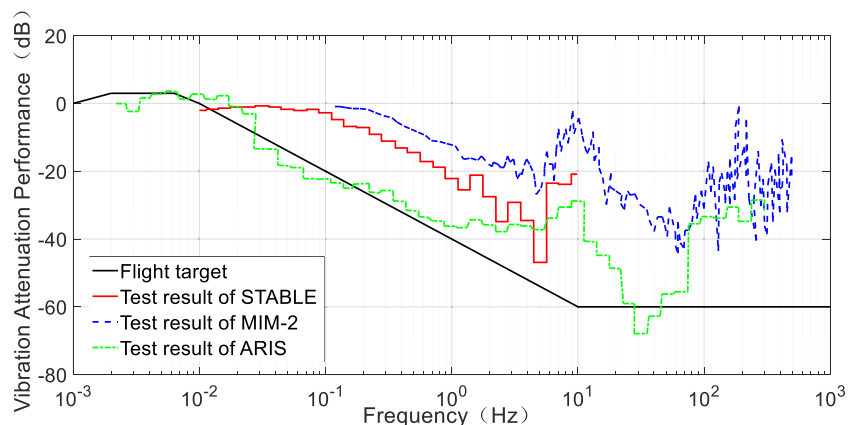
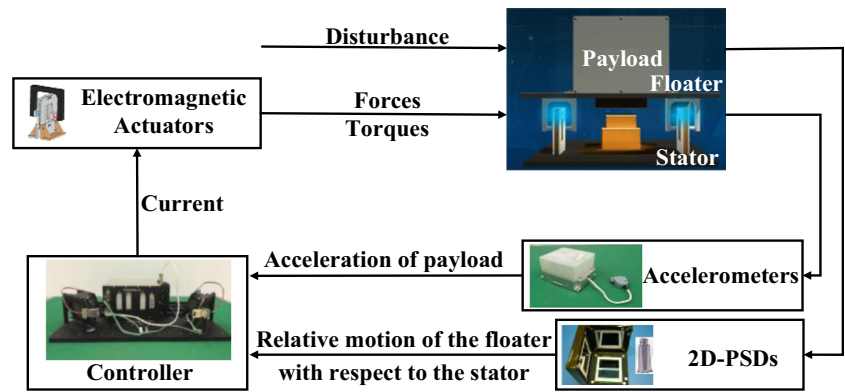


Fig. 3 System working principle of MAIS



integrated isolator modules, each of which was comprised of a dual axis actuator, two single axis accelerometers, two axes of implicit position sensing, and control electronics. The integration of sensing, actuation, and avionics into a single package was the key novel feature of g-LIMIT that allowed for a more highly reconfigurable, compact design of general utility. MIM (Duval and Tryggvason 2000) was the first active vibration isolation system developed by CSA (Canadian Space Agency), accumulating more than 2500 h of operation supporting experiments in liquid metal diffusion, crystal growth, glass nucleation, and protein crystal growth on the MIR Space Station. MIM-2 (Casgrain et al. 2004) was an upgraded version of MIM. The major improvements were in the system electronics and the electro-magnetic actuators. The electronics were redesigned to reduce the level of electronic noise, and they were completely modular to allow for on-orbit maintenance. The electromagnetic actuator design was also modified to reduce the position-related nonlinearity in the forces that the actuators apply to the isolated platform. This improved the stability of the control algorithms. MVIS (Labib et al. 2010) was the third generation of MIM technology. The MVIS was designed to actively isolate the ESA’s (European Space Agency) FCE from vibrations in the ISS. The flight model of the MIVS was tested by an aircraft parabolic flight on

the Airbus A300 ZERO-G. The MVIS performance was then estimated using test results paired with a high fidelity MVIS simulation. MIMBU (Herring and Gregory 2000) was the fourth generation of MIM technology. MIMBU was a two-stage standalone system installed into an EXPRESS rack. The system provided measurement of accurate acceleration data for both the floater and the stator in isolating, forced vibration, and latched modes. This facilitated experiments designed to evaluate the effects of spacecraft g-jitter on the results. Figure 2 illustrates the effects of the attenuation of vibration amplitude at variable frequencies achieved by STABLE, MIM-2 and ARIS.

The Microgravity Active vibration Isolation System (MAIS), designed by the Technology and Engineering Center for Space Utilization, Chinese Academy of Sciences, is the first device designed and operated by China to demonstrate and test advanced technology of microgravity active vibration isolation in space (Ren et al. 2010). It has been verified in the DLR 27th parabolic flight campaign (Zhang et al. 2017). A further space flight test was conducted on board the China’s first cargo-spacecraft TZ-1. The objectives of MAIS in the TZ-1 mission are summarized as: (1) to provide required microgravity environment for the payload, (2) to verify the technology of magnetic levitation control in space and (3) to test the performance indices of

Fig. 4 Flight model of MAIS



Table 1 Flight tests of MAIS in the TZ-1 mission

Platform	Attitude mode	Test periods (all in 2017)	Code name
TG-2 + TZ-1	three-axis stabilized orientation	April 29–May 12 June 1–June 3	GZS
TG-2 + TZ-1	yaw steering	May 12–May 23 May 29–June 1	GZY
TZ-1	three-axis stabilized orientation	June 23–July 1 July 22–August 26	TZS
TZ-1	yaw steering	August 26–September 4	TZY

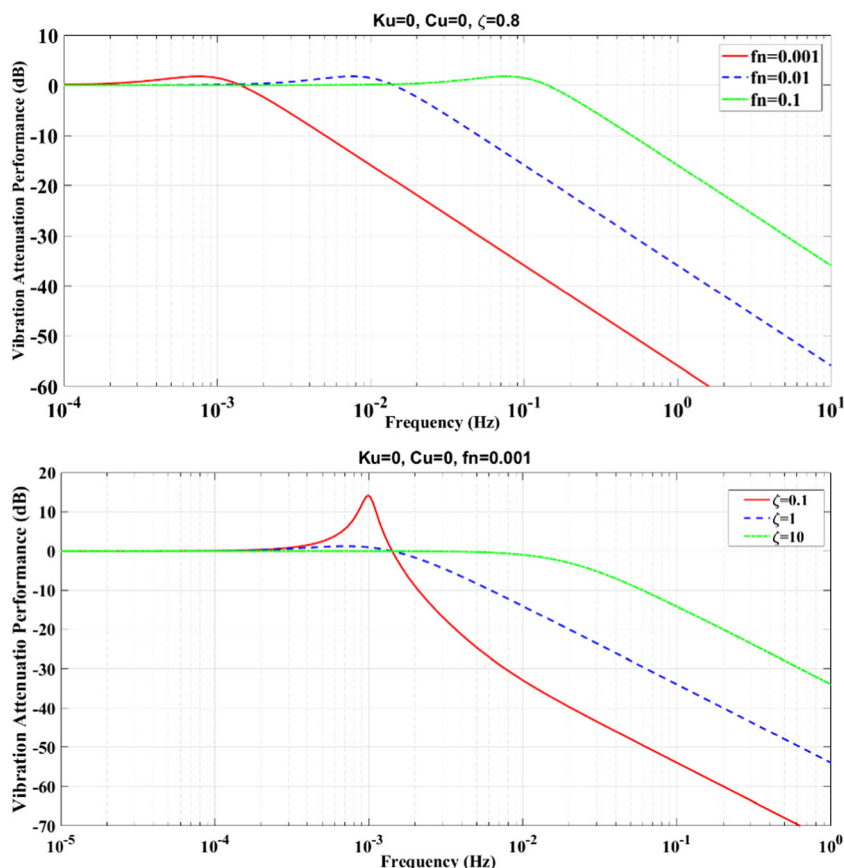
Table 2 Unification of the sensitive direction of the acceleration data

Spacecraft-fixed coordinate system	Floater-fixed coordinate system	Stator-fixed coordinate system	TISS-fixed coordinate system
-Z	X	X	Y
-Y	Y	Y	Z
-X	Z	Z	X

MAIS. This article is to present the flight test results of MAIS. The content of this article is organized as follow. Second section introduces the system configuration of MAIS on TZ-1. Third section describes the performance indices of MAIS’s flight test, which are specifically referred to as microgravity acceleration and vibration

attenuation under control. Fourth section describes the microgravity acceleration measurements of the spacecraft platforms in the TZ-1 mission, followed by the flight test results of MAIS that are presented in fifth section. The contributing factors to the microgravity level limit and vibration attenuation under control are also

Fig. 5 Relationship between controller parameters and vibration attenuation performance



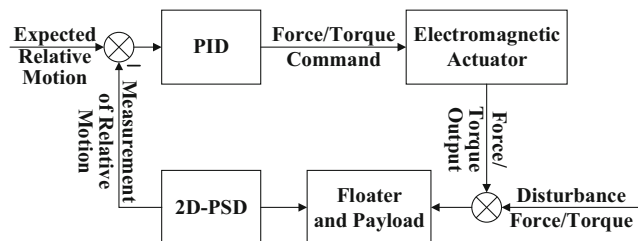


Fig. 6 Position control scheme of MAIS

analyzed in “Flight test results of MAIS and relevant analysis” section. The experiences and lessons from the flight results of MAIS in the TZ-1 mission are summarized in sixth section, and seventh section presents brief summaries.

The System Configuration of MAIS on TZ-1

MAIS is composed of a stator fixed on a spacecraft and a floater (on which the payloads is mounted) levitated close to the stator. A bundle of umbilical cables for power supply and data transmission are the only mechanical links between the floater and the stator. The system working principle is shown in Fig. 3, which aims to minimize the amplitude of the non-gravitational acceleration of the floater in a specific range of frequencies. The key lies in the integration of measurement, control and actuation. The relative motion of the floater with respect to the stator are sensed by 2D-PSDs, and the acceleration of the payload (or the floater) are measured by accelerometers. In accordance with these high precision measurement, the controller is designed to calculate the required forces and torques generated by electromagnetic actuators.

The flight model of MAIS onboard TZ-1 is as shown in Fig. 4. The main body consists of a stator and a floater. The microgravity control performance of MAIS’s prototype model

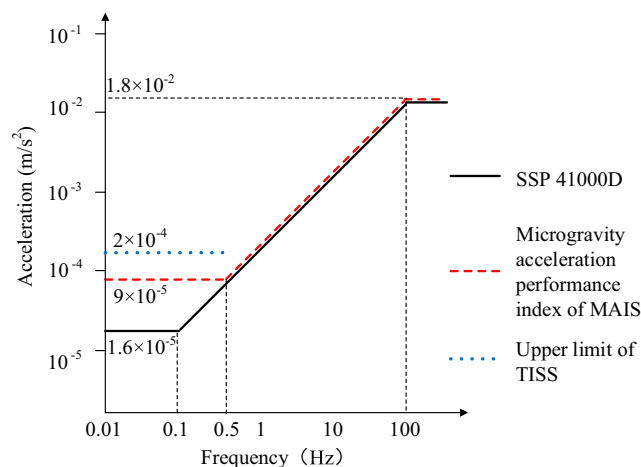


Fig. 7 Requirements of vibratory acceleration on ISS and on MAIS

Table 3 Comparison of VP1 and VP2

Calculation methods	Spatiotemporal characteristics	Source and accuracy of acceleration data
VP1	Same space Different time	Electrostatic levitation accelerometers, 10^{-10} m/s ²
VP2	Different space Same time	MAIS, 5×10^{-5} m/s ²

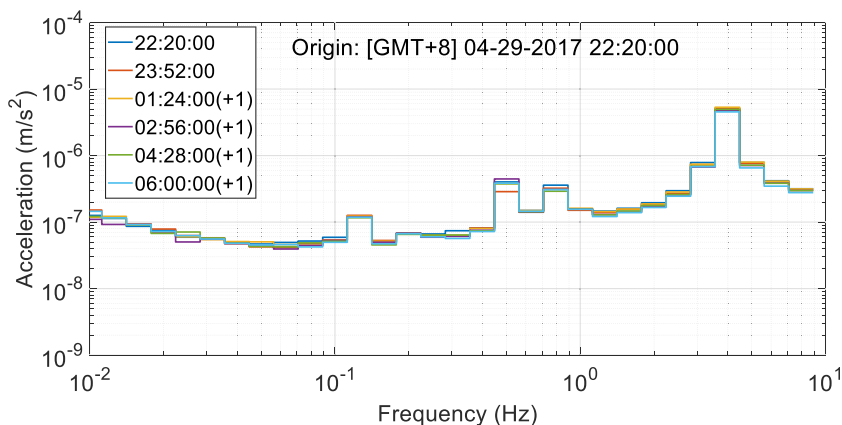
was fully simulated and tested by computer simulation and engineering tests, including the tests of the 3-DOF (Degree Of Freedom) motion by air-bearing platform levitation and 6-DOF motion by aircraft parabolic flight. Simulation and test results verify the accuracy of the control strategy design, effectiveness of the control algorithms, and performance of the entire control system. The details of these simulation and tests could be found in an earlier paper (Liu et al. 2018).

The payload mounted on the floater is a set of high-precision electrostatic levitation accelerometers, designed by Huazhong University of Science and Technology. The electrostatic levitation accelerometers are used for Test of Inverse-Square-law in Space (TISS). The electrostatic levitation accelerometers are designed to have the measurement accuracy of 10^{-10} m/s² and can accurately measure the microgravity acceleration of MAIS during the TZ-1 mission. When the floater is fixed to the stator, data read from the electrostatic levitation accelerometers represents the acceleration of both the floater and the stator. When the floater is levitated to the stator under control, data read from the electrostatic levitation accelerometers represents the acceleration of the floater with vibration isolation.

Operating Modes

TZ-1 was launched on April 20, 2017, performed docks with the manned space laboratory TG-2 for three times, and finally reentered atmosphere on September 22, 2017. According to the different spacecraft platforms, four modes for operating MAIS were conducted during the TZ-1 mission, as shown in Table 1. The flight tests of MAIS’s microgravity performance are implemented on two types of spacecraft platforms, termed “TG-2 + TZ-1” and “TZ-1”. “TG-2 + TZ-1” is referred to as the two-body platform when TG-2 and TZ-1 are docked with each other. “TZ-1” represents the Tianzhou-1 cargo-spacecraft when it orbits the Earth alone. Each type of platform has two attitude orientation modes: three-axis stabilized orientation mode and yaw steering mode. Yaw steering mode is to maintain nadir-pointing and sun tracking by continuously controlling the yaw angle of the spacecraft (Runge 1991). For simplify, “TG-2 + TZ-1” in the three-axis stabilized orientation and yaw steering modes are abbreviated as GZS and GZY, respectively, and “TZ-1” in the three-axis

Fig. 8 RMS acceleration in the one-third octave of GZS in the direction of MAIS-X



stabilized orientation and yaw steering modes are abbreviated as TZS and TZY, respectively. The total operating periods of MAIS on board the TZ-1 mission are approximately 85 d, including 16 d on GZS, 15 d on GZY, 44.5 d on TZS, and 9.5 d on TZY.

Acceleration Measurements

The acceleration measurement data of MAIS on board the TZ-1 mission consists of three types: the acceleration of the floater, the stator, and the electrostatic levitation accelerometers. The sensitive direction of the measurement data should be unified, as shown in Table 2.

The three axes of the floater-fixed and the stator-fixed coordinate system are the same. Therefore, the floater-fixed and the stator-fixed coordinate system can generally be called the MAIS-fixed coordinate system, where the three axes are denoted as MAIS-X, MAIS-Y, and MAIS-Z. When the spacecraft is under the three-axis stabilized orientation mode, MAIS-X corresponds to the normal direction of the orbital plane, MAIS-Y corresponds to the radial direction of the orbital plane (direction between the spacecraft and the center of the Earth), and MAIS-Z corresponds to the tangential direction of the orbital plane (flight direction of the spacecraft). The acceleration measurement data are all recorded by distinct accelerometers and are used to derive the control

performances (microgravity acceleration and vibration attenuation) that will be described in “Microgravity performance indices in flight test” section.

Dynamics Modelling and Controller Design

Dynamics modelling and controller design is briefly introduced to analysis the vibration isolation fundamentals. Firstly, the rotational motion of the floater and the stator are ignored, and their translational motion equations are established. Then, a simple PD controller is designed and a closed loop transfer function from the stator’s microgravity acceleration to the floater’s microgravity acceleration is obtained. Finally, the controller parameters are expressed by the system mass, stiffness, and damping ratio, which determine the vibration attenuation performance.

Based on Newton’s Second Law, the dynamic models of the floater and the stator can be expressed as

$$\begin{aligned}
 m_F \ddot{\mathbf{x}}_F &= \mathbf{F}_{gF} + \mathbf{F}_c + \mathbf{F}_u + \mathbf{F}_d \\
 m_S \ddot{\mathbf{x}}_S &= \mathbf{F}_{gS} + m_S \cdot \mathbf{a}_{mS}
 \end{aligned}
 \tag{1}$$

where m_F and m_S are the mass of the floater and the stator, respectively, \mathbf{x}_F and \mathbf{x}_S are the vector from the center of the Earth to the centroid of the floater and the vector from the center of the Earth to the centroid of the stator, respectively,

Fig. 9 RMS acceleration in the one-third octave of GZS in the direction of MAIS-Y

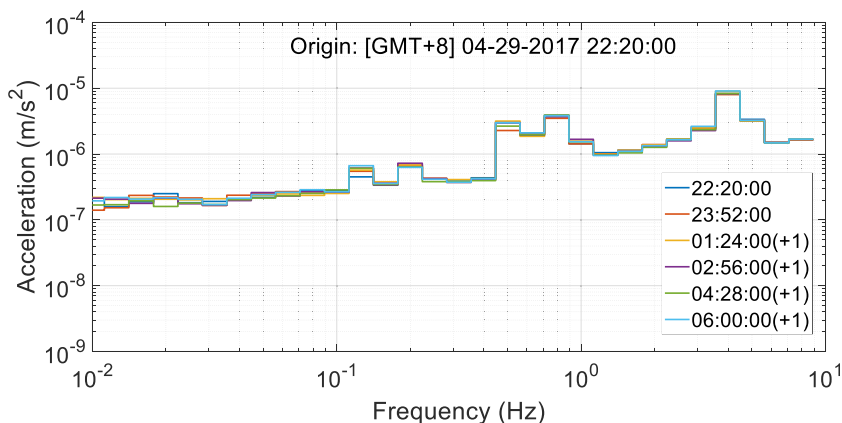
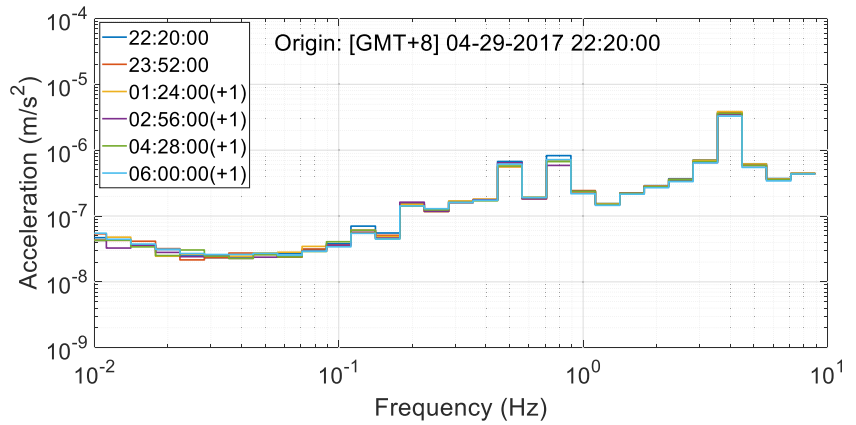


Fig. 10 RMS acceleration in the one-third octave of GZS in the direction of MAIS-Z



x_F and x_S are the modulus of \mathbf{x}_F and \mathbf{x}_S , respectively, $\ddot{\mathbf{x}}_F$ and $\ddot{\mathbf{x}}_S$ are the two-order derivatives of \mathbf{x}_F and \mathbf{x}_S with respect to the geocentric inertial coordinate system, respectively, \mathbf{F}_{gF} ($= -m_F \cdot \mu_E \cdot \mathbf{x}_F / x_F^3$) and \mathbf{F}_{gS} ($= -m_S \cdot \mu_E \cdot \mathbf{x}_S / x_S^3$) are the gravitational attraction of the floater and the stator, respectively, $\mu_E (= 3.986 \times 10^5 \text{ km}^3/\text{s}^2)$ is the gravitational constant of the Earth, \mathbf{F}_c is the control force calculated by the controller and generated by electromagnetic actuators, \mathbf{F}_u is the disturbance force caused by umbilical cables, \mathbf{F}_d is the sum of disturbance forces (\mathbf{F}_u excluded), \mathbf{a}_{mS} is the microgravity acceleration of the stator, that is, the microgravity acceleration of the spacecraft platform.

The disturbance force \mathbf{F}_u could be modelled as a second-order damping system. Ignoring the rotational motion of the floater and the stator, \mathbf{F}_u can be expressed as

$$\mathbf{F}_u = -\mathbf{K}_u \cdot \mathbf{x}_e - \mathbf{C}_u \cdot \dot{\mathbf{x}}_e + \mathbf{F}_b \tag{2}$$

where \mathbf{K}_u and \mathbf{C}_u are the stiffness and damping matrices, respectively, $\mathbf{x}_e (= \mathbf{x}_F - \mathbf{x}_S)$ is the position error of the floater with respect to the stator, $\dot{\mathbf{x}}_e$ is the derivative of \mathbf{x}_e with respect to the stator-fixed coordinate system, respectively, \mathbf{F}_b is the disturbance force caused by umbilical cables at the reference position where \mathbf{x}_e equals zero. \mathbf{K}_u and \mathbf{C}_u are very small and difficult to measure

accurately, so they are not considered in the controller design. The PD controller can be expressed as

$$\mathbf{F}_c = -\mathbf{K}_c \cdot \mathbf{x}_e - \mathbf{C}_c \cdot \dot{\mathbf{x}}_e - \mathbf{F}_b \tag{3}$$

where \mathbf{K}_c and \mathbf{C}_c are the controller parameters.

The equation of the floater’s relative motion with respect to the stator can be derived by considering Eqs. (1)~(3).

$$\begin{aligned} \ddot{\mathbf{x}}_e + (\mathbf{C}_c + \mathbf{C}_u) / m_F \cdot \dot{\mathbf{x}}_e + (\mathbf{K}_c + \mathbf{K}_u) / m_F \cdot \mathbf{x}_e \\ = \mathbf{F}_{gF} / m_F - \mathbf{F}_{gS} / m_S + \mathbf{F}_d / m_F - \mathbf{a}_{mS} \end{aligned} \tag{4}$$

where $\mathbf{F}_{gF} / m_F (= -\mu_E \cdot \mathbf{x}_F / x_F^3)$ and $\mathbf{F}_{gS} / m_S (= -\mu_E \cdot \mathbf{x}_S / x_S^3)$ are determined by \mathbf{x}_F and \mathbf{x}_S , respectively. For the earth orbit spacecraft, $x_F \geq 6400 \text{ km}$ and $x_S \geq 6400 \text{ km}$. Because the vector $\mathbf{x}_e (= \mathbf{x}_F - \mathbf{x}_S)$ is usually limited to $\pm 10 \text{ mm}$, $|\mathbf{F}_{gF} / m_F - \mathbf{F}_{gS} / m_S| \leq 3 \times 10^{-8} \text{ m/s}^2$. Under the assumed condition $\mathbf{F}_{gF} / m_F \approx \mathbf{F}_{gS} / m_S = \ddot{\mathbf{x}}_g$, the Laplace transformation of Eq. (4) at each DOF can be expressed as

$$\begin{aligned} [\tilde{x}_F(s) - \tilde{x}_g(s)] s^2 + (\tilde{C}_c + \tilde{C}_u) / m_F [\tilde{x}_F(s) - \tilde{x}_g(s)] s \\ + (\tilde{K}_c + \tilde{K}_u) / m_F [\tilde{x}_F(s) - \tilde{x}_g(s)] \\ = (\tilde{C}_c + \tilde{C}_u) / m_F [\tilde{x}_S(s) - \tilde{x}_g(s)] s \\ + (\tilde{K}_c + \tilde{K}_u) / m_F [\tilde{x}_S(s) - \tilde{x}_g(s)] + \tilde{F}_d(s) / m_F \end{aligned} \tag{5}$$

Fig. 11 RMS acceleration in the one-third octave of different spacecraft platforms in the direction of MAIS-X

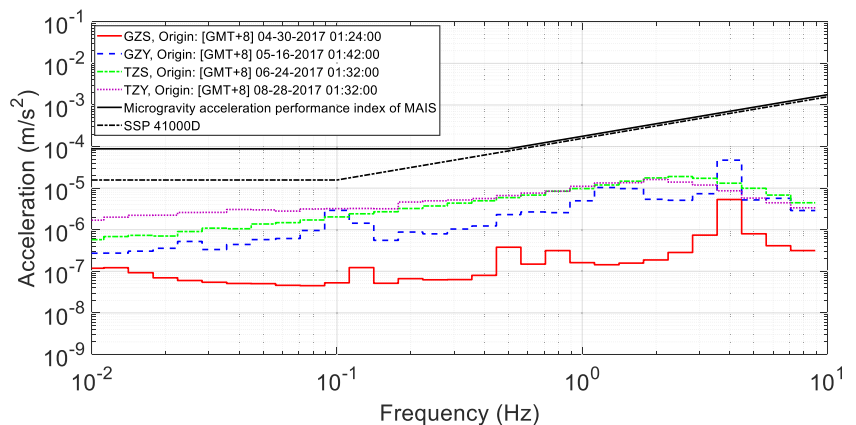
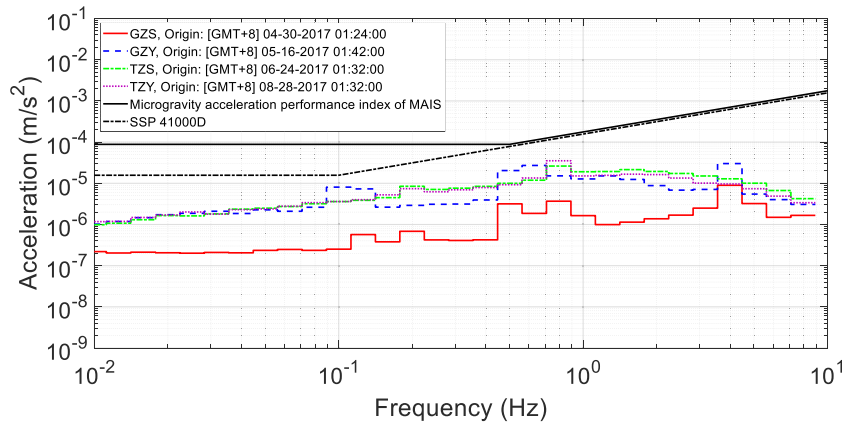


Fig. 12 RMS acceleration in the one-third octave of different spacecraft platforms in the direction of MAIS-Y



where \tilde{X} represents the component of the vector X at each DOF.

Ignoring the disturbance force F_d , the closed loop transfer function from the stator’s microgravity acceleration to the floater’s microgravity acceleration at each DOF is expressed as

$$\begin{aligned} \tilde{G}(s) &= \frac{\ddot{\tilde{a}}_{mF}(s)}{\ddot{\tilde{a}}_{mS}(s)} = \frac{\ddot{\tilde{x}}_F(s) - F_{gF}(s)/m_F}{\ddot{\tilde{x}}_S(s) - F_{gS}(s)/m_S} \\ &\approx \frac{\tilde{x}_F(s) \cdot s^2 - \tilde{x}_g(s) \cdot s^2}{\tilde{x}_S(s) \cdot s^2 - \tilde{x}_g(s) \cdot s^2} \\ &= \frac{(\tilde{C}_c + \tilde{C}_u)s + (\tilde{K}_c + \tilde{K}_u)}{m_F s^2 + (\tilde{C}_c + \tilde{C}_u)s + (\tilde{K}_c + \tilde{K}_u)} \end{aligned} \tag{6}$$

The closed loop transfer function $\tilde{G}(s)$ can be equivalent to a set of first-order differentiation element and oscillating element, so $\tilde{G}(s)$ can be also expressed as

$$\tilde{G}(s) = \frac{2\omega_n\zeta s + \omega_n^2}{s^2 + 2\omega_n\zeta s + \omega_n^2} \tag{7}$$

where ω_n is the natural frequency and ζ is damping ratio. Compared with Eq. (6), the controller parameters are expressed as

$$\begin{aligned} \tilde{K}_c &= m_F \omega_n^2 - \tilde{K}_u \\ \tilde{C}_c &= 2m_F \omega_n \zeta - \tilde{C}_u \end{aligned} \tag{8}$$

where the mass of the floater m_F can be measured easily. The stiffness and damping of umbilical cables, \tilde{K}_u and \tilde{C}_u , are very difficult to measure accurately. The stiffness and damping of umbilical cables are required to be small enough to be ignored. The controller parameters expressed by m_F , $\omega_n (=2\pi f_n)$, and ζ determine the closed loop transfer function $\tilde{G}(s)$ and the vibration attenuation performance, as shown in Fig. 5.

Due to the coupling of translational motion and rotational motion, the interference of umbilical cables and the influence of filters, the actual test results of vibration attenuation performance are different from those shown in Fig. 5. Two control schemes, a position control scheme and an acceleration control scheme, are designed to minimize the amplitude of the non-gravitational acceleration of the floater, and to control the floater to track the stator limited to ± 10 mm in translation and $\pm 2^\circ$ in rotation. The position control scheme takes the translational and rotational position of the floater with respect to the stator as feedback. The acceleration control scheme takes both the translational and rotational position of the floater with respect to the stator and the microgravity acceleration of the floater as feedback. If the noise of the floater’s accelerometers is lower than the amplitude of the acceleration of the floater

Fig. 13 RMS acceleration in the one-third octave of different spacecraft platforms in the direction of MAIS-Z

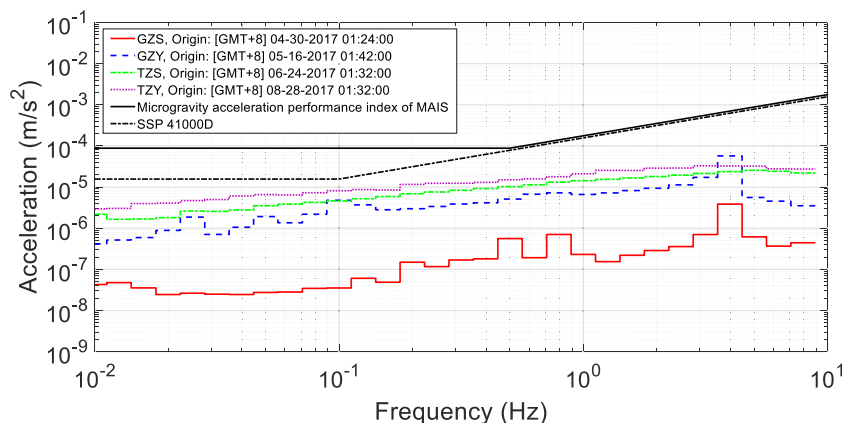
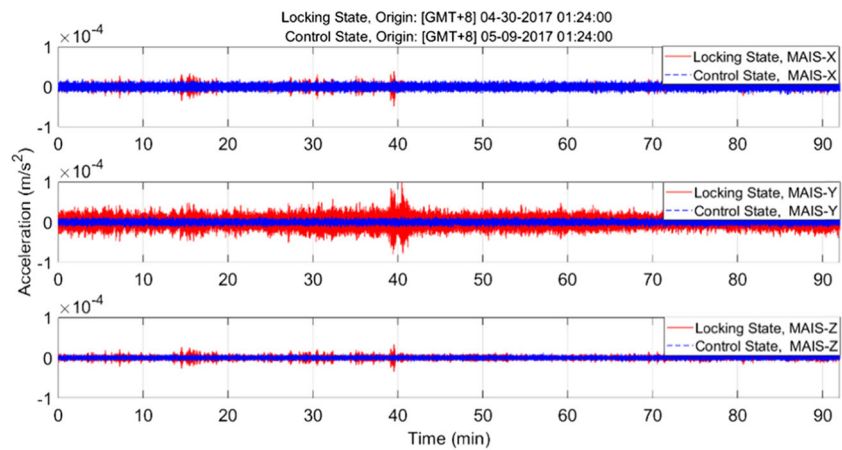


Fig. 14 Microgravity acceleration of MAIS under control on GZS



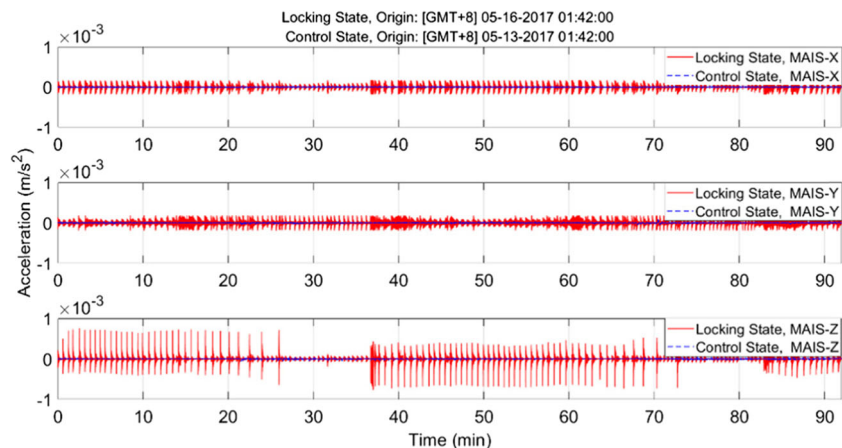
under the position control scheme, the acceleration control scheme should provide a higher-level microgravity environment than the position control scheme. However, for the TZ-1 mission the noise of the floater’s accelerometers ($5 \times 10^{-5} \text{ m/s}^2$) is even higher than the amplitude of the acceleration of the spacecraft ($10^{-7} - 10^{-6} \text{ m/s}^2$). When compared to the acceleration control scheme, the effect of the position control scheme was better during the TZ-1 mission. The flight results of MAIS under the position control scheme are only presented in this paper. The position control scheme is shown in Fig. 6.

The PID controller for position control scheme is expressed as

$$\begin{bmatrix} \mathbf{F}_c \\ \mathbf{M}_c \end{bmatrix} = -\mathbf{K}_P \begin{bmatrix} \mathbf{x}_e \\ \boldsymbol{\theta}_e \end{bmatrix} - \mathbf{K}_D \begin{bmatrix} \dot{\mathbf{x}}_e \\ \dot{\boldsymbol{\theta}}_e \end{bmatrix} - \mathbf{K}_I \int \begin{bmatrix} \mathbf{x}_e \\ \boldsymbol{\theta}_e \end{bmatrix} dt - \begin{bmatrix} \mathbf{F}_b \\ \mathbf{M}_b \end{bmatrix} \quad (9)$$

where \mathbf{F}_c and \mathbf{M}_c are the control force and control torque, respectively, \mathbf{x}_e and $\boldsymbol{\theta}_e$ are the position error and attitude angle error of the floater with respect to the stator, respectively, $\dot{\mathbf{x}}_e$ and $\dot{\boldsymbol{\theta}}_e$ are the derivatives of \mathbf{x}_e and $\boldsymbol{\theta}_e$ with respect to the stator-fixed coordinate system, respectively, \mathbf{K}_P , \mathbf{K}_D and \mathbf{K}_I are the parameters of the PID controller, and \mathbf{F}_b and \mathbf{M}_b are the force and torque caused by umbilical cables at the expected relative position, respectively, and they can be calibrated through the position control system of MAIS when it is in orbit.

Fig. 15 Microgravity acceleration of MAIS under control on GZY



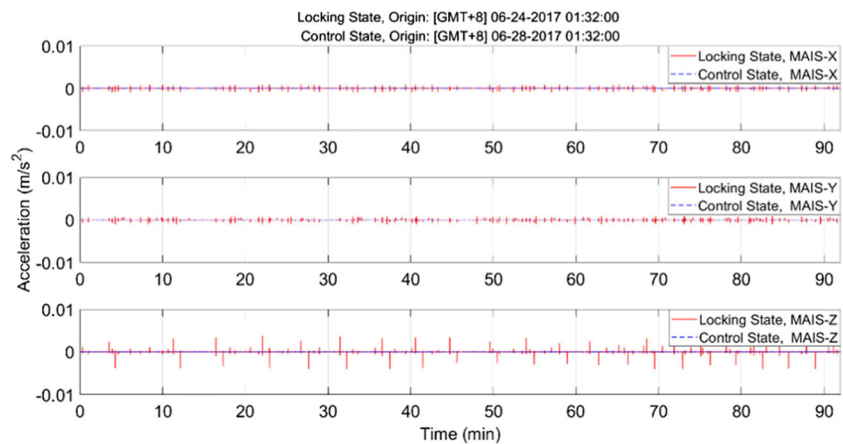
Microgravity Performance Indices in Flight Test

Microgravity Acceleration

Microgravity acceleration is a fundamental performance index to represent the microgravity environment of payloads under control of vibration isolation devices. The requirement of vibratory acceleration on ISS, SSP 41000D, is defined as follows (Delombard et al. 2005): the vibratory acceleration of payloads at structural mounting interfaces averaged over 100 s should be limited to RMS (Root Mean Square) acceleration magnitude in the one-third octave not exceeding the black line in Fig. 7.

The requirement of vibratory acceleration of MAIS on TZ-1 is shown as the red dashed line in Fig. 7. The relationship between the requirement of microgravity level a and vibration frequency f is approximately modeled as follows: 1) $a \leq 9 \times 10^{-5} \text{ m/s}^2$ if $f < 0.5 \text{ Hz}$, 2) $a \leq f \times 18 \times 10^{-5} \text{ m/s}^2$ if $f = 0.5 - 100 \text{ Hz}$, and 3) $a \leq 1.8 \times 10^{-2} \text{ m/s}^2$ if $f > 100 \text{ Hz}$. Providing a high-level microgravity environment for the payload is an important objective of MAIS in the TZ-1 mission. The measurement

Fig. 16 Microgravity acceleration of MAIS under control on TZS



range of the electrostatic levitation accelerometers is shown as the blue dotted line in Fig. 7, which is $2 \times 10^{-4} \text{ m/s}^2$.

The performance index of microgravity acceleration are usually determined by scientific payloads. The microgravity level under control depends on the vibratory acceleration of the spacecraft and the vibration attenuation performance of vibration isolation devices. Therefore, vibration attenuation rather than microgravity acceleration is used to evaluate the control performance of vibration isolation devices.

Vibration Attenuation

The vibration attenuation performance is defined as the attenuation of the residual acceleration of a payload under control with respect to the vibratory acceleration of the spacecraft platform at the installation position of the payload. MAIS is controlled so as to isolate from the vibration on TZ-1 at frequencies above 0.1 Hz. The performance index of vibration attenuation of MAIS on TZ-1 is defined as follows: (1) For vibration at frequencies smaller than 0.1 Hz, the vibration attenuation is not required, and the maximum vibration magnification at the resonant frequency should not exceed 3 dB. (2) For vibration in the frequency band of 0.1–10 Hz, the

vibration attenuation is from 0 to 40 dB. (3) For vibration at frequencies larger than 10 Hz, the vibration attenuation is –40 dB.

In accordance with the definition of vibration attenuation performance, the two accelerations of the payload under control and the spacecraft at the same space position should be measured at the same time. However, it is impossible to measure the two accelerations at the same space and time. Two approximate calculation methods of vibration attenuation performance of MAIS on TZ-1 are proposed, VP1 and VP2 for short. VP1 is the attenuation of acceleration of the payload under control with respect to the acceleration of the payload under locking at different time periods. The state of locking is that the floater is locked by a locking mechanism fixed on the stator. The acceleration of the payload under locking represents the microgravity acceleration of TZ-1 at the installation position of the payload. VP1 can be expressed as

$$VP1 = 20 \times \lg \frac{a_{TISS_Control}}{a_{TISS_Lock}} \quad (10)$$

where $a_{TISS_Control}$ and a_{TISS_Lock} are the accelerations of the payload under control and locking, respectively. Both $a_{TISS_Control}$ and a_{TISS_Lock} represent the frequency-domain microgravity levels computed by Fourier transformation of the time-

Fig. 17 Microgravity acceleration of MAIS under control on TZY

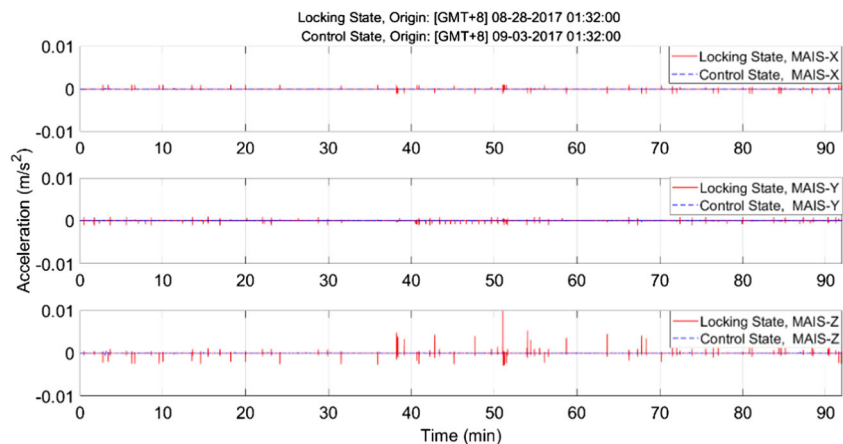
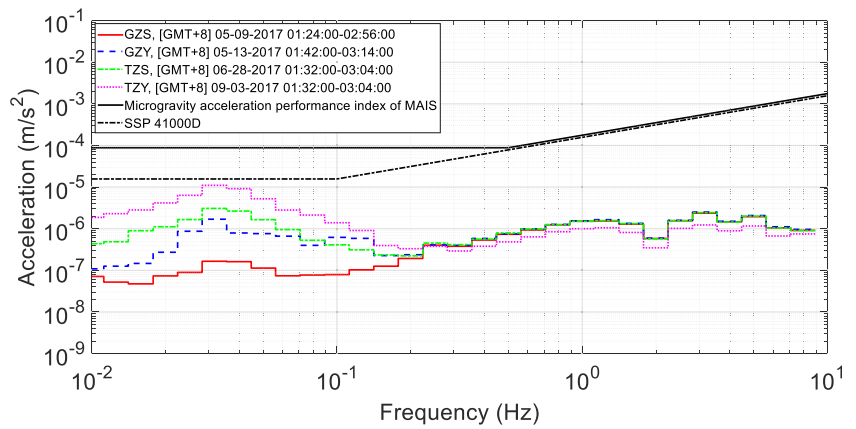


Fig. 18 RMS acceleration in the one-third octave of MAIS under control in the direction of MAIS-X



domain counterparts. VP2 is the attenuation of acceleration of the floater under control with respect to the acceleration of the stator under control at the same time. VP2 can be expressed as

$$VP2 = 20 \times \lg \frac{a_{Floater_Control}}{a_{Stator_Control}} \quad (11)$$

where $a_{Floater_Control}$ and $a_{Stator_Control}$ are the accelerations of the floater under control and the stator under control, respectively. Both $a_{Floater_Control}$ and $a_{Stator_Control}$ represent the frequency-domain microgravity levels computed by Fourier transformation of the time-domain counterparts.

From the perspective of spatiotemporal characteristics, VP1 has the characteristics of same space and different time, while VP2 has the characteristics of different space and same time. From the perspective of source and accuracy of acceleration data, VP1 is based on the acceleration data of the electrostatic levitation accelerometers with the accuracy of 10^{-10} m/s^2 , while VP2 is based on the acceleration data of the floater and stator with the accuracy of $5 \times 10^{-5} \text{ m/s}^2$. The comparison of VP1 and VP2 is shown in Table 3.

During the TZ-1 mission the noise of the MAIS’s accelerometers ($5 \times 10^{-5} \text{ m/s}^2$) was higher than the amplitude of the acceleration of the spacecraft ($10^{-8} - 10^{-6} \text{ m/s}^2$). Therefore, VP2 cannot be used to calculate the vibration attenuation performance of MAIS on TZ-1. Fortunately, the spacecraft’s

microgravity levels averaged over an orbit period (about 92 min) are consistent over different time periods, which shows that VP1 is feasible.

Microgravity Acceleration Measurements of Spacecraft Platforms

According to the definition of SSP 41000D, the RMS acceleration in the one-third octave of the payload under locking averaged over 92 min (an orbit period) is evaluated as the microgravity acceleration of the spacecraft platforms, as shown in Figs. 8, 9, and 10. In these figures “Origin” represents the beginning of the data segment, and “[GMT + 8]” represents the Greenwich Mean Time plus 8 h. Each line in these legends is the RMS acceleration in the one-third octave of the 92 min length data, and the numbers of the time are the beginning of the 92 min length data, and “+1” represents the day after the origin day.

These figures show that the microgravity levels of GZS averaged over 92 min are consistent through different time periods. Similar results can also be observed on GZY, TZS, and TZY. Therefore, the calculation method VP1 can be used to calculate the vibration attenuation performance of MAIS on

Fig. 19 RMS acceleration in the one-third octave of MAIS under control in the direction of MAIS-Y

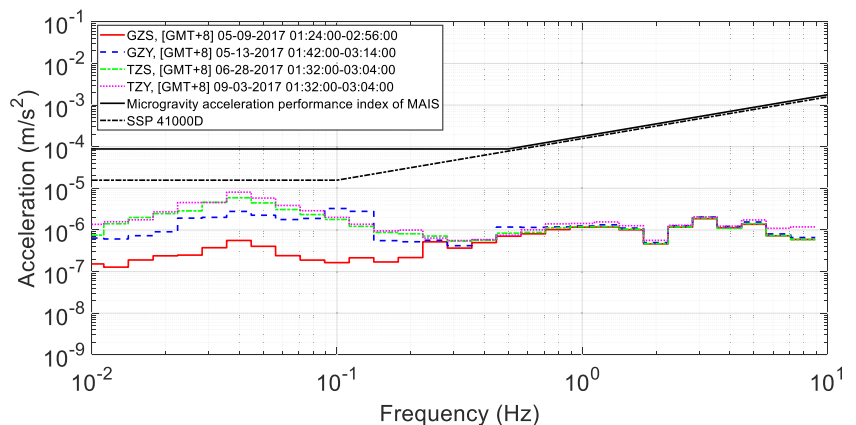
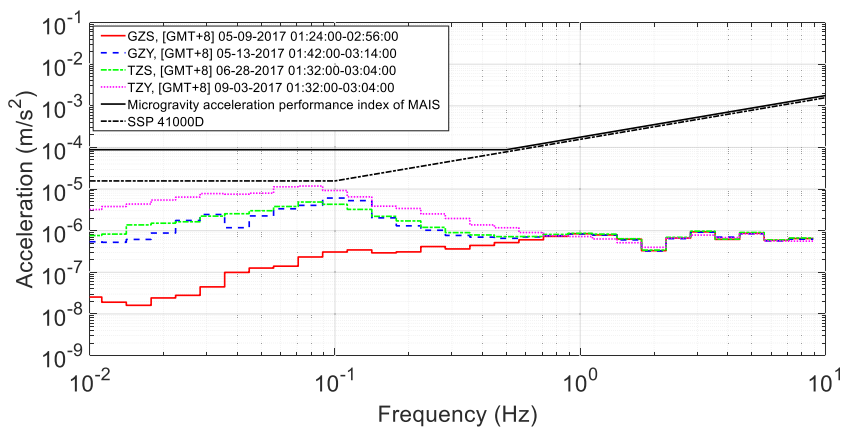


Fig. 20 RMS acceleration in the one-third octave of MAIS under control in the direction of MAIS-Z



board the TZ-1 mission. The microgravity levels of different spacecraft platforms are shown in Figs. 11, 12, and 13.

The microgravity accelerations of the four spacecraft platforms (GZS, GZY, TZS and TZY) are measured in orbit, and the sequence of the microgravity level from high to low is GZS, GZY, TZS and TZY. The microgravity accelerations of the four spacecraft platforms all reached the microgravity level required by MAIS. The goal of providing a high-level microgravity environment for the payload can be even achieved without active vibration isolation. However, the other goals of verifying the technology of magnetic levitation control in 6 DOF and testing the performance indices of MAIS should be operated under active control during the TZ-1 mission. The measurement data of the four spacecraft platforms is valuable for the task design and performance index determination of MAIS-like devices.

Flight Test Results of MAIS and Relevant Analysis

The Performance of Microgravity Acceleration

The microgravity acceleration of MAIS with the PID controller (Fig. 6 and Eq. (9)) and the same control

parameters on the four spacecraft platforms are shown in Figs. 14, 15, 16, and 17.

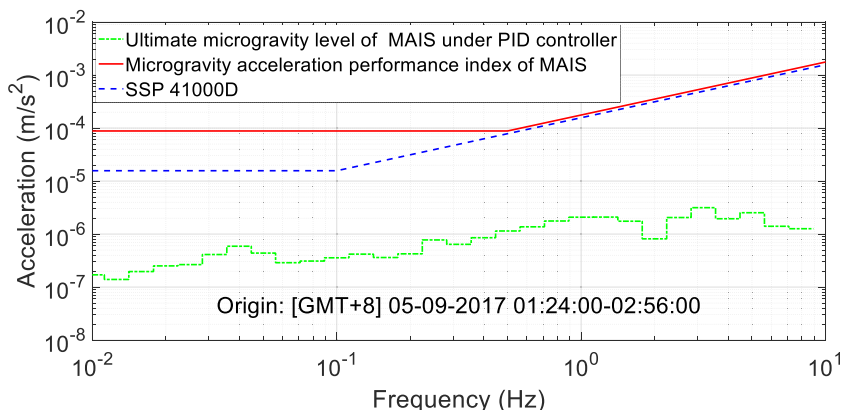
The microgravity acceleration performance of MAIS is expressed as the RMS acceleration in the one-third octave of the payload under control averaged over 92 min, as shown in Figs. 18, 19, and 20.

Figures 18, 19, and 20 show that the performance of microgravity acceleration on the four spacecraft platforms are:

- 1) different at frequencies lower than 0.2 Hz and almost the same in the frequency band of 0.2–10 Hz in the directions of MAIS-X and MAIS-Y;
- 2) and different at frequencies lower than 0.7 Hz and almost the same in the frequency band of 0.7–10 Hz in the direction of MAIS-Z.

If a spacecraft is in the state of high-level microgravity or even free fall, the microgravity acceleration of MAIS under control is referred to as microgravity level limit. The microgravity level limit of MAIS is determined by the device itself and is independent of the spacecraft. The same microgravity accelerations in the frequency band of 0.7–10 Hz indicate the existence of the microgravity level limit of MAIS with the PID controller. The flight test results show that the microgravity level limit of MAIS with the PID controller is approximate

Fig. 21 Microgravity level limit of MAIS with the PID controller



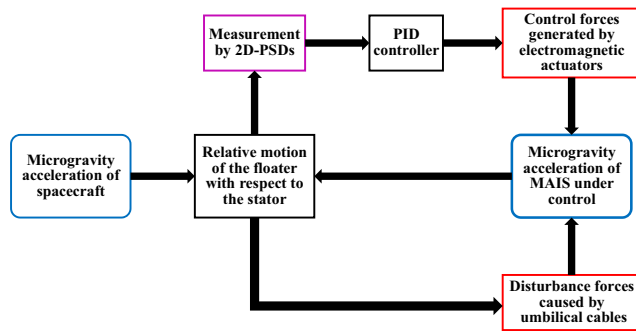


Fig. 22 Factors relating to the MAIS’s microgravity acceleration with the PID controller

$10^{-7} - 10^{-6} \text{ m/s}^2$ in the frequency band of 0.01–10 Hz, as shown in Fig. 21.

The microgravity acceleration depends on the sum of non-gravitational forces (all forces except gravity). The non-gravitational forces acting on the floater of MAIS mainly include the control forces generated by the electromagnetic actuators and the disturbance forces caused by the umbilical cables. The control forces are calculated by the PID controller based on the measurement of 2D-PSDs. The factors relating to the microgravity acceleration of MAIS with the PID controller are shown in Fig. 22.

Figure 22 shows that the contributing factors to the microgravity level limit of MAIS with the PID controller include the measurement noise of 2D-PSDs, the output force noise of electromagnetic actuators, and disturbance forces of the umbilical cables. Therefore, the core technology which will improve the microgravity level limit of MAIS under control consists of improving the accuracy of 2D-PSDs and electromagnetic actuators and reducing the disturbance forces of the umbilical cables. Wireless energy transmission and wireless communication are feasible alternatives to umbilical cables.

The Performance of Vibration Attenuation

The vibration attenuation performance of MAIS is calculated using VP1. The flight test results of MAIS with the PID

controller (Fig. 6 and Eq. (9)) and the same control parameters on the four spacecraft platforms are shown in Fig. 23.

Figure 23 shows that the flight test results of the vibration attenuation performance of MAIS on the four spacecraft platforms are different, because of the existence of the microgravity level limit of MAIS under control. The sequence of the vibration attenuation performance from high to low is arranged as TZY, TZS, GZY and GZS, and it is contrary to the sequence of the microgravity level of the four spacecraft platforms. The vibration attenuation performance of MAIS will be usually better under the worse microgravity environment. Then the best test results of the vibration attenuation performance at different frequencies (Fig. 23) are selected as the vibration attenuation performance of MAIS in the TZ-1 mission, as shown in Fig. 24.

The vibration attenuation performance of MAIS in the TZ-1 mission almost meets the performance index of vibration attenuation except at frequencies higher than 1 Hz. Because MAIS on all four spacecraft platforms reaches the microgravity level limit at frequencies higher than 0.2 Hz, the ability of MAIS to isolate vibration at this frequency band can not be verified in orbit. The vibration attenuation performance of MAIS in a computer simulation is calculated based on the acceleration measurements of the payload in orbit, as shown in Fig. 25.

The blue line in Fig. 25 represents the vibration attenuation performance of MAIS in a computer simulation under the acceleration measurements of the payload in orbit, which is consistent with the flight result (the red line in Fig. 25). If the acceleration of the spacecraft platform in the computer simulation is magnified by 100 times relative to the acceleration measurements of the payload in orbit, the vibration attenuation performance of MAIS in the computer simulation is shown as the green line in Fig. 25. At frequencies higher than 0.2 Hz the green line has a better vibration attenuation performance than the blue line, and the only difference is that the microgravity accelerations of the spacecraft platform in the computer simulation are different. This verifies the accuracy

Fig. 23 Vibration attenuation performance of MAIS on the four spacecraft platforms

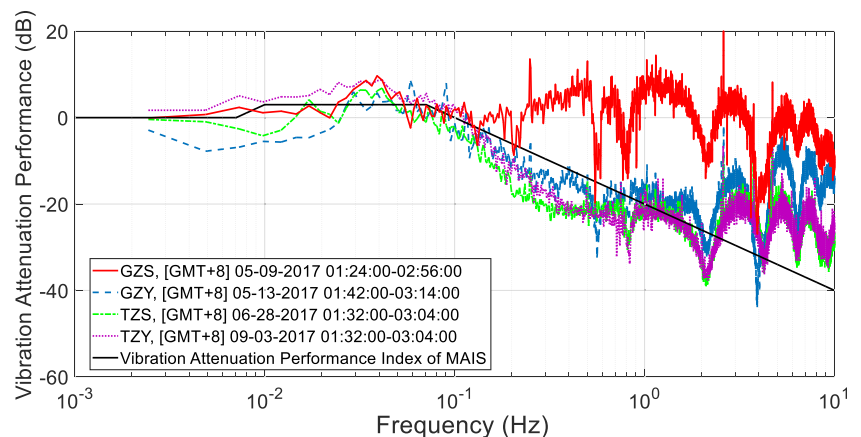
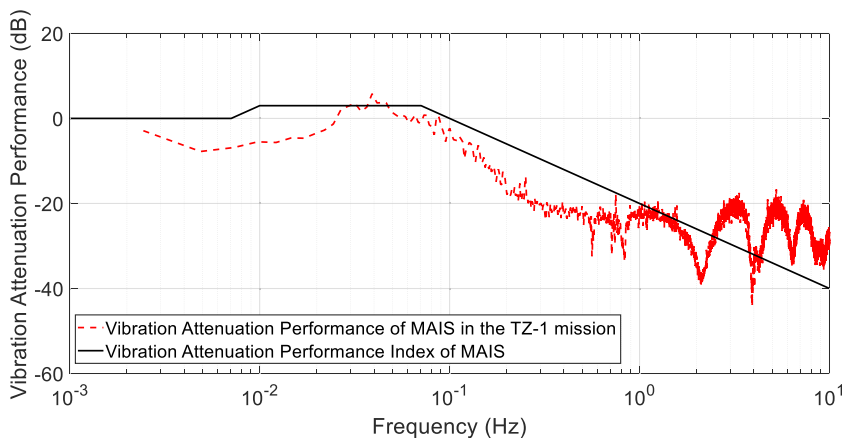


Fig. 24 Vibration attenuation performance of MAIS in the TZ-1 mission



of the analysis about the vibration attenuation performance of MAIS.

Lessons Learned

The flight test results of MAIS during the TZ-1 mission are presented. The flight test results verified the success of MAIS. The control system including state estimation and control laws achieved the required microgravity precision. In particular, the position control scheme for MAIS was proven to be effective. The microgravity acceleration performance of MAIS under control was 1–2 orders of magnitude better than the performance index of the microgravity acceleration of MAIS during the TZ-1 mission. The vibration attenuation performance of MAIS almost met the performance index of the vibration attenuation except at frequencies higher than 1 Hz. The experiences and lessons learned from the flight test of MAIS on board the TZ-1 mission are as follows:

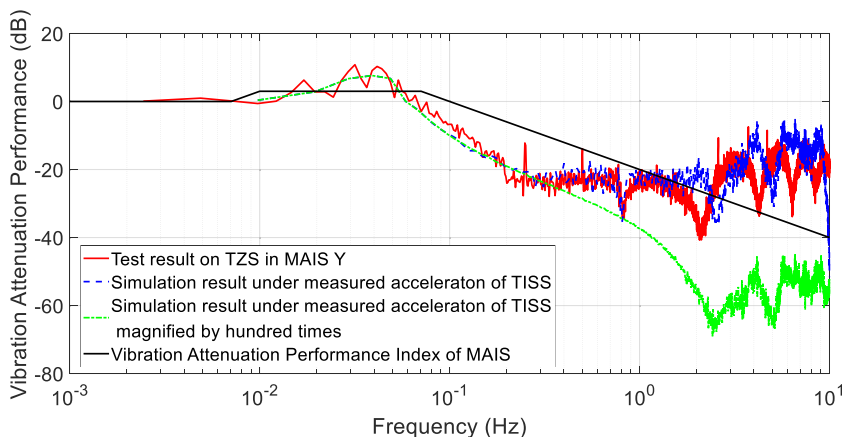
- (1) The microgravity accelerations of the spacecraft platform (GZS, GZY, TZS or TZY) averaged over 92 min (orbit period) are consistent at different time periods. RMS acceleration in the one-third octave averaged over

92 min is suitable for the evaluation of the microgravity accelerations of the spacecraft platforms and MAIS.

- (2) The calculation method VP1 based on the acceleration measurements of the payload under control and under locking is appropriate for calculating the vibration attenuation performance of MAIS on board the TZ-1 mission.
- (3) The microgravity level limit of MAIS with the PID controller is 10^{-7} – 10^{-6} m/s² in the frequency band of 0.01–10 Hz. The main contributing factors are the measurement noise of 2D-PSDs, the output force noise of electromagnetic actuators, and disturbance forces of the umbilical cables.
- (4) The flight test results of vibration attenuation performance depend on the microgravity acceleration of the spacecraft platform and the microgravity level limit of MAIS. However, the vibration attenuation performance of MAIS is independent of the spacecraft. When the microgravity acceleration of MAIS under control doesn't reach its microgravity level limit, the vibration attenuation performance of MAIS can be truly tested.

MAIS was designed to provide a high-level microgravity environment for scientific payloads. The microgravity acceleration is an important performance index of a MAIS-like

Fig. 25 Comparison of vibration attenuation performance of MAIS in flight test and computer simulation



device, which can be improved by the enhancement of the vibration attenuation performance and the microgravity level limit. The improvement of the accuracy of 2D-PSDs and electromagnetic actuators and the reduction of the disturbance forces of umbilical cables are effective to achieve higher-level performance indices.

Summaries

This article presents flight test results of MAIS in the TZ-1 mission. By evaluating the control performances of microgravity acceleration and vibration attenuation, the flight test results show that MAIS performed well in orbit even though no acceleration measurement feedback is present in the controller. Some experiences and lessons learned are summarized, which is beneficial in developing MAIS-like devices on board China's Space Station in the near future.

Acknowledgements The authors gratefully acknowledge Zebing Zhou, Yanzheng Bai, Shuchao Wu, Shaobo Qu, Jianbo Yu, et al., who are from Huazhong University of Science and Technology. They provided the measured acceleration data of the payload that is the key to obtain the flight test results. The authors would also like to thank Anping Wang, Boqi Kang, Lingcai Song, Mengxi Yu, Peng Yang, Shimeng Lv, Weijia Ren, Xiaoru Sang, Yanlin Zhou, Yongkang Zhang and Yu'e Gao, who have contributed significantly to the MAIS project.

Open Access This article is distributed under the terms of the Creative Commons Attribution 4.0 International License (<http://creativecommons.org/licenses/by/4.0/>), which permits unrestricted use, distribution, and reproduction in any medium, provided you give appropriate credit to the original author(s) and the source, provide a link to the Creative Commons license, and indicate if changes were made.

References

Casgrain, C., Dejmek, M., Ruel, S., et al.: The canadian space agency microgravity sciences program of overview. In: 42nd AIAA Aerospace Sciences Meeting and Exhibit, Aerospace Sciences Meetings, Reno, Nevada, U.S.A. (2004)

- Delombard, R., Hrovat, K., Kelly, E., et al.: Interpreting the international space station microgravity environment. In: 43rd AIAA Aerospace Sciences Meeting and Exhibit, Reno, Nevada, U.S.A. (2005)
- Duval, W.M.B., Tryggvason, B.V.: Effects of G-Jitter on interfacial dynamics of two miscible liquids: application of MIM. In: 37th Aerospace Sciences Meeting and Exhibit, Reno, Nevada, U.S.A. (2000)
- Ederberg, D., Boucher, R., Schenck, D., et al.: Results of the STABLE microgravity vibration isolation flight experiment. In: 37th Aerospace Sciences Meeting and Exhibit, Reno, Nevada, U.S.A. (1996)
- Grodsinsky, C.M., Whorton, M.S.: Survey of active vibration isolation systems for microgravity applications. *J. Spacecr. Rocket.* **37**(5), 586–596 (2000)
- Herring, R.A., Gregory, P.R.: CSA's ISS MIM Base unit for the EXPRESS rack. *AIP Conf. Proc.* **504**(1), 611–613 (2000)
- Labib, M., Piontek, D., Valsecchi, N., et al.: The fluid science laboratory's microgravity vibration isolation subsystem overview and commissioning update. In: SpaceOps 2010 Conference Delivering on the Dream Hosted by NASA Marshall Space Flight Center and Organized by AIAA, Huntsville, Alabama, U.S.A. (2010)
- Liu, W., Zhang, Y., Li, Z., et al.: Control performance simulation and tests for microgravity active vibration isolation system onboard the Tianzhou-1 cargo-spacecraft. *Astrodynamics.* (2018). <https://doi.org/10.1007/s42064-018-0028-7>
- NASA Facts: Active Rack Isolation System (ARIS). In: Expedition 2, ISS Mission 6A, STS-101 Space Shuttle Flight, pp. Pub 8–40412. National Aeronautics and Space Administration, Marshall Space Flight Center, Huntsville, Alabama 35812 (2005)
- Ren, W., Li, Z., Gao, Y.: Microgravity active vibration isolation system for space science in China. In: 61st International Astronautical Congress, IAC-10-a.2.5.10, Prague, (2010)
- Runge, H.: Benefits of antenna yaw steering for SAR. In: 11th Annual International Geoscience and Remote Sensing Symposium, IGARS S'91, 1, 257–261 (1991)
- Whorton, M.S.: g-LIMIT: a microgravity vibration isolation system for the international space station. In: 2001 Conference and exhibit on international space station utilization, Cape Canaveral, FL, U.S.A. (2001)
- Zhang, Y., Dong, W., Liu, W., et al.: Verification of the microgravity active vibration isolation system based on parabolic flight. *Microgravity Sci. Technol.* **29**, 415–426 (2017)